

The photochemical generation of heterobimetallic complexes containing carbon disulfide

Peter V. Broadhurst, Nicholas E. Leadbeater,* Jack Lewis and Paul R. Raithby

Department of Chemistry, Lensfield Road, Cambridge, UK CB2 1EW

Photochemistry has been used to generate a number of heterobimetallic complexes containing $\pi + \sigma$ CS₂ bridging groups. Broad-band UV photolysis of tetrahydrofuran (thf) solutions of [M(CO)₆] (M = Cr, Mo or W) with [Fe(CO)₂(PR₃)₂(η^2 -CS₂)] (R = Et or Ph) leads to the formation of the bimetallic complexes [(PR₃)₂(CO)₂Fe-(μ - η^2 : η^1 -CS₂)M(CO)₅]. Photolysis of acetonitrile solutions of [Os₃(CO)₁₂] with [Fe(CO)₂(PR₃)₂(η^2 -CS₂)] leads to [(PR₃)₂(CO)₂Fe(μ - η^2 : η^1 -CS₂)Os₃(CO)₁₁]. Photolysis of a thf solution of (PEt₃)₂(CO)₂Fe(μ - η^2 : η^1 -CS₂)M(CO)₅] with PEt₃ results in the formation of the phosphine-substituted complex [(PPh₃)₂(CO)₂Fe(μ - η^2 : η^1 -CS₂)M(CO)₄-(PEt₃)]. Single-crystal X-ray diffraction has been used to determine the molecular structures of [(PPh₃)₂(CO)₂Fe-(μ - η^2 : η^1 -CS₂)W(CO)₅], [(PEt₃)₂(CO)₂Fe(μ - η^2 : η^1 -CS₂)Os₃(CO)₁₁] and [(PPh₃)₂(CO)₂Fe(μ - η^2 : η^1 -CS₂)Cr(CO)₄(PEt₃)].

The interaction of heteroallene molecules such as carbonyl sulfide (COS), carbon disulfide (CS₂) and carbon dioxide (CO₂) with transition metals has become an area of increased research interest.^{1,2} Firstly, petrochemical feedstocks have sulfur-containing compounds as impurities which poison many hetero- or homo-geneous catalysts used in processing.³ If the behaviour of these impurities with transition-metal centres is established, an insight into the mechanism for poisoning could be gained and attempts made to prevent it. In addition, heteroallenes show interesting chemistry undergoing a number of transformations such as insertion, dimerisation and disproportionation.^{1a}

Work in our research group has focused on the photochemical generation of carbon disulfide-containing complexes of the Group 8 transition metals and their subsequent reaction chemistry. To date, many of the Group 8 transition-metal-CS₂ complexes reported have been prepared by thermolysis or pyrolysis routes. Although illustrating interesting chemistry, in many cases the CS₂ moiety does not remain intact, often forming, for example, carbide, sulfide, CS, C₂S₂, CS₃ and C₂S₄ groups in various co-ordination modes.⁴ Photochemistry offers a simple, and often highly selective, route to organometallic compounds, overcoming large enthalpy barriers.^{5,6} As a consequence, it is often possible to prepare complexes that are otherwise inaccessible by conventional thermochemical routes. We have studied the photochemical behaviour of [Fe(CO)₅] **1** and [Fe(CO)₃(PR₃)₂] (R = Et **2a** or Ph **2b**) with CS₂ and the reaction chemistry of the photolysis products has been investigated.

Results and Discussion

Photolysis of [Fe(CO)₅] **1** and [Fe(CO)₃(PR₃)₂] (R = Et **2a** or Ph **2b**) with CS₂

Broad-band UV photolysis of a hexane solution of [Fe(CO)₅] **1** containing CS₂ leads rapidly to the formation of a brown precipitate, which is insoluble in organic solvents. Due to this insolubility, characterisation of the reaction product has not been possible. The aim of this experiment was to prepare the η^2 -CS₂ co-ordinated complex [Fe(CO)₄(η^2 -CS₂)], analogous to the olefin complex [Fe(CO)₄(η^2 -C₂H₄)]. Since carbon disulfide is not as good a π -acceptor ligand as ethene, the formation of the η^2 -CS₂ complex is not possible using the present experimental methods due to the inherent instability of the complex.

Attention was turned to phosphine-substituted mononuclear iron carbonyl complexes since, by replacing carbonyl groups by

phosphines, η^2 -co-ordinating ligands can be stabilised. This is as a result of a strong increase in binding energy which is consistent with increased π -back donation in the phosphine-substituted complex. Indeed, *ab initio* calculations⁷ have shown that replacement of carbonyl groups by phosphines in iron(0) carbon disulfide complexes results in an increased overlap between the interacting orbitals on Fe and CS₂, this being concomitant with deformation of the CS₂ geometry which itself enhances the effect.

Irradiation of a tetrahydrofuran (thf) solution of [Fe(CO)₃(PR₃)₂] (R = Et **2a** or Ph **2b**) with CS₂ leads to the η^2 -CS₂ co-ordinated complex [Fe(CO)₂(PR₃)₂(η^2 -CS₂)] (R = Et **3a** or Ph **3b**) [equation (1)] as characterised by comparison of the



spectral data with those reported previously for **3b**.⁸ The *trans* stereochemistry of **3a** and **3b** was evident from the ¹H NMR parameters (see below). The disulfide products are formed in high yields, this being a marked improvement on the conventional synthetic routes of either refluxing [Fe₂(CO)₉] and tertiary phosphine in CS₂ as the solvent^{8,9} or ligand exchange reactions.¹⁰ The bonding of the CS₂ group is considered to be analogous to the Dewar-Chatto model proposed for alkenes. The net structural effect of σ donation from the π molecular orbitals (MO) on CS₂ to the iron and back donation from iron to a π^* MO on the disulfide is a distortion of the CS₂ moiety towards the geometry observed in the first excited state.¹⁰ Concomitant with this is a lengthening of the CS bonds as shown by the decrease in CS stretching frequency from 1535 cm⁻¹ in free carbon disulfide (ν_2)¹¹ to 1116 in **3a**. From comparison of this value with those for analogous η^2 -CS₂ complexes reported in the literature,⁸⁻¹⁰ a correlation between ν_{CS} and the electronic properties of the phosphorus ligand is found, phosphite ligands having higher ν_{CS} values than analogous phosphines. Although informative, data for the C-S stretching frequency must be considered carefully since coupling with other ligand modes is often severe in the ν_{CS} region of the infrared spectrum¹² with the result that significance cannot be placed on absolute values of frequencies reported here or in other CS₂-containing molecules.¹⁰ The analogous complex [Fe(CO)₂(PMe₃)(PPh₃)(η^2 -CS₂)] **3c** has been characterised crystallographically and shows definitively both the lengthening of the CS bonds and also significant deformation of the CS₂ moiety, the S-C-S angle being 139°.¹⁰

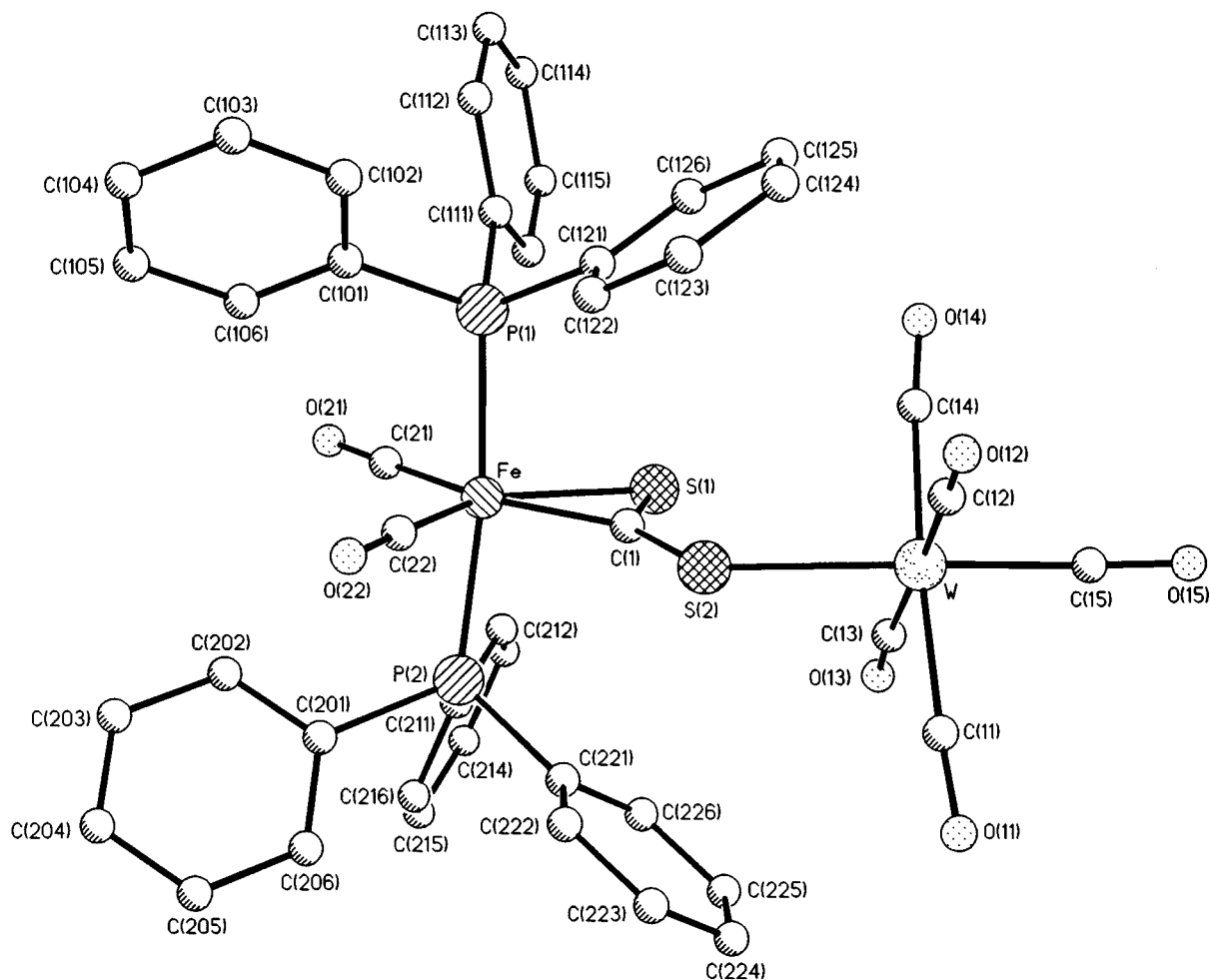


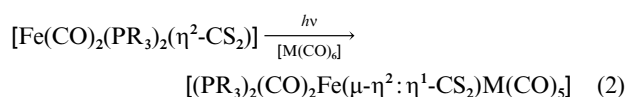
Fig. 1 The molecular structure of $[(\text{PPh}_3)_2(\text{CO})_2\text{Fe}(\mu\text{-}\eta^2\text{:}\eta^1\text{-CS}_2)\text{W}(\text{CO})_5]$ **7b**

The $\eta^2\text{-CS}_2$ co-ordinated complexes **3a** and **3b** are stable in solution for extended periods. In addition, the complexes are stable to displacement of CS_2 by phosphines, this being in contrast to that of $[\text{Fe}(\text{CO})_4(\eta^2\text{-C}_2\text{H}_4)]^5$ in which the alkene moiety is substituted readily. If a solution of **3a** or **3b** is heated under an atmosphere of carbon monoxide, the CS_2 group is replaced by CO to yield **2a** or **2b**.

The reaction chemistry of $[\text{Fe}(\text{CO})_2(\text{PEt}_3)_2(\eta^2\text{-CS}_2)]$ and $[\text{Fe}(\text{CO})_2(\text{PPh}_3)_2(\eta^2\text{-CS}_2)]$ with mononuclear and cluster carbonyl fragments

The reaction chemistry of $[\text{Fe}(\text{CO})_2(\text{PEt}_3)_2(\eta^2\text{-CS}_2)]$ **3a** and $[\text{Fe}(\text{CO})_2(\text{PPh}_3)_2(\eta^2\text{-CS}_2)]$ **3b** with $[\text{M}(\text{CO})_6]$ ($\text{M} = \text{Cr}, \text{Mo}$ or W) and $[\text{Os}_3(\text{CO})_{12}]$ has been investigated. The unco-ordinated sulfur in transition-metal η^2 -co-ordinated CS_2 complexes is highly nucleophilic and is therefore susceptible to attack by electrophiles.¹³ This is demonstrated clearly by reaction with methyl iodide yielding, in the case of **3a**, $[\text{Fe}(\text{CO})_2(\text{PEt}_3)_2(\eta^2\text{-CS}_2\text{Me})]^+$ **4a**.

Broad-band UV photolysis of a thf solution of complex **3a** with $[\text{M}(\text{CO})_6]$ ($\text{M} = \text{Cr}, \text{Mo}$ or W) leads to the formation of the CS_2 -bridged complex $[(\text{PEt}_3)_2(\text{CO})_2\text{Fe}(\mu\text{-}\eta^2\text{:}\eta^1\text{-CS}_2)\text{M}(\text{CO})_5]$ ($\text{M} = \text{Cr}$ **5a**, Mo **6a** or W **7a**) [equation (2)] as characterised



initially by IR and ^1H NMR spectroscopy. Analogous complexes **5b**, **6b** or **7b** are formed with **3b**.

The complexes are formed presumably by attack of **3a** on $[\text{M}(\text{CO})_5(\text{thf})]$, the latter intermediate being formed photo-

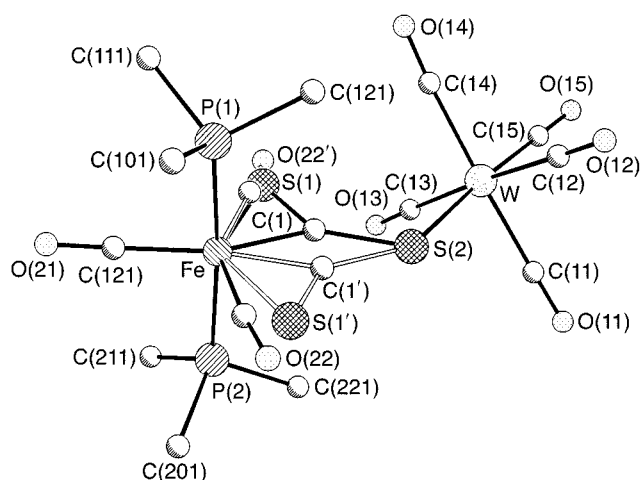


Fig. 2 The molecular structure of $[(\text{PPh}_3)_2(\text{CO})_2\text{Fe}(\mu\text{-}\eta^2\text{:}\eta^1\text{-CS}_2)\text{W}(\text{CO})_5]$ **7b** showing the crystallographic disorder of the CS_2 and one CO ligand (phenyl rings removed for clarity)

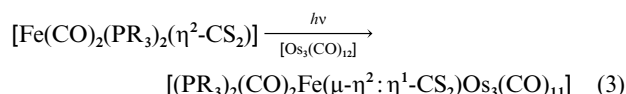
chemically. The IR spectrum of the products shows five bands in the CO stretching region this being in agreement with local C_{4v} symmetry at the M centre (three ν_{CO} bands) and retention of the local C_{2v} symmetry of the $[\text{Fe}(\text{CO})_2(\text{PR}_3)_2(\eta^2\text{-CS}_2)]$ fragment. Slight splitting of one of the bands due to the M centre is observed, this being attributed to the slight deviation from a regular octahedral geometry. This assignment has been confirmed by the determination of the molecular structure of $[(\text{PPh}_3)_2(\text{CO})_2\text{Fe}(\mu\text{-}\eta^2\text{:}\eta^1\text{-CS}_2)\text{W}(\text{CO})_5]$ **7b** by a single-crystal X-ray diffraction study (Figs. 1 and 2). Selected bond lengths and angles are shown in Table 1. The molecular structure shows disorder in the CS_2 group and one of the carbonyl groups at

Table 1 Selected bond lengths and angles for complex **7b**

W–S(2)	2.531(4)	W–C(11)	2.02(2)
W–C(12)	2.017(17)	W–C(13)	2.044(18)
W–C(14)	2.039(16)	W–C(15)	1.977(16)
Fe–P(1)	2.293(4)	Fe–P(2)	2.289(4)
Fe–S(1)	2.299(1)	Fe–S(1')	2.300(1)
Fe–C(1)	1.850(1)	Fe–C(1')	1.850(1)
Fe–C(21)	1.790(15)	Fe–C(22)	1.79(2)
Fe–C(22')	1.800(1)	S(1)–C(1)	1.669(9)
C(1)–S(2)	1.760(1)	C(1')–S(1')	1.576(12)
C(1')–S(2)	1.760(1)	C(11)–O(11)	1.15(2)
C(12)–O(12)	1.134(16)	C(13)–O(13)	1.15(2)
C(14)–O(14)	1.138(16)	C(15)–O(15)	1.161(16)
C(21)–O(21)	1.151(16)	C(22)–O(22)	1.17(3)
C(22')–O(22')	1.150(1)		
C(11)–W–S(2)	89.7(4)	C(12)–W–S(2)	83.5(4)
C(13)–W–S(2)	93.8(4)	C(14)–W–S(2)	95.6(4)
C(15)–W–S(2)	174.6(4)	W–C(11)–O(11)	175.2(15)
W–C(12)–O(12)	179.0(15)	W–C(13)–O(13)	176.1(14)
W–C(14)–O(14)	175.4(13)	W–C(15)–O(15)	177.9(13)
W–S(2)–C(1)	109.0(2)	W–S(2)–C(1')	151.0(4)
S(2)–C(1)–S(1)	138.7(3)	S(2)–C(1')–S(1')	136.2(4)
S(2)–C(1)–Fe	139.8(4)	S(2)–C(1')–Fe	139.8(4)
C(1)–S(1)–Fe	52.7(1)	C(1)–Fe–S(1)	45.9(3)
C(1)–Fe–P(1)	94.1(6)	C(1)–Fe–P(2)	94.0(6)
C(1)–Fe–C(21)	153.7(5)	C(1)–Fe–C(22)	99.1(7)
C(1')–S(1')–Fe	53.1(1)	C(1')–Fe–P(1)	90.3(12)
C(1')–Fe–P(2)	92.2(12)	C(1')–Fe–C(21)	167.2(5)
C(1')–Fe–C(22')	87.5(16)		

iron which precludes an assessment of the bond parameters in **7b**. It is, however, clear from the structure that the CS₂ group interacts in a π manner with the iron centre and in a σ manner with the tungsten; this bridging bonding mode being denoted as $\pi + \sigma$. Of all the bridging modes of CS₂ structurally characterised, the $\pi + \sigma$ motif is relatively uncommon.¹⁴ The reasons why **7b** adopts this configuration are not clear but the stability of the π bond between iron and CS₂ and the mild reaction conditions used in the coupling reaction with [W(CO)₆] may be significant factors. Although not statistically different at the 3 σ level, the W–C(15) bond, at 1.977(16) Å, is apparently shorter than the other W–C (O) bonds, average 2.02(4) Å. This is indicative of the increased back donation as a result of the replacement of a *trans* carbonyl by a *trans* σ bonding sulfur which is not competing for the electron density available for back donation. This effect has been reported previously for sulfur-substituted Group 6 carbonyls.^{15,16} The other bond lengths and the angles in the W(CO)₅S moiety are unexceptional, a very slight distortion from a regular octahedral geometry being observed.

Broad-band UV photolysis of an acetonitrile solution of complex **3a** with [Os₃(CO)₁₂] leads to the formation of the mononuclear-cluster linked compound [(PEt₃)₂(CO)₂Fe(μ - η^2 : η^1 -CS₂)Os₃(CO)₁₁] **8a** [equation (3)] as characterised

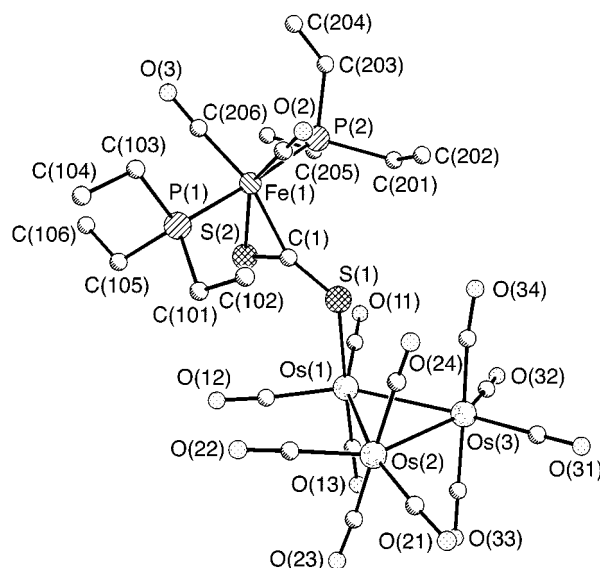


initially by IR and ¹H NMR spectroscopy. An analogous compound **8b** is formed with **3b**. Again, the *trans* stereochemistry of the iron centre is unchanged in the reaction and the bonding of the CS₂ is π to the iron centre and σ to one of the osmium atoms of the trinuclear cluster. It is presumed that the reaction occurs by way of an attack of **3a** or **3b** on [Os₃(CO)₁₁(MeCN)], the latter formed by photosubstitution of a carbonyl group for acetonitrile.¹⁷

The molecular structure of **8a** has been determined by single-crystal X-ray diffraction (Fig. 3) and selected bond lengths and angles are presented in Table 2. The $\pi + \sigma$ co-ordination of CS₂

Table 2 Selected bond lengths and angles for complex **8a**

Os(1)–Os(2)	2.886(2)	Os(1)–Os(3)	2.883(1)
Os(2)–Os(3)	2.877(2)	Os(1)–C(11)	1.861(3)
Os(1)–C(12)	1.91(3)	Os(1)–C(13)	1.85(3)
Os(1)–S(1)	2.461(6)	Os(2)–C(21)	1.86(3)
Os(2)–C(22)	1.92(3)	Os(2)–C(23)	1.83(3)
Os(2)–C(24)	1.93(3)	Os(3)–C(31)	1.92(2)
Os(3)–C(32)	1.86(4)	Os(3)–C(33)	1.93(3)
Os(3)–C(34)	1.83(4)	C(11)–O(11)	1.17(4)
C(12)–O(12)	1.16(3)	C(13)–O(13)	1.15(3)
C(1)–S(1)	1.64(2)	C(1)–S(2)	1.65(2)
Fe–C(1)	1.95(2)	Fe–S(2)	2.341(7)
Fe–C(2)	1.81(1)	Fe–C(3)	1.803(19)
Fe–P(1)	2.270(9)	Fe–P(2)	2.284(10)
C(2)–O(2)	1.091(1)	C(3)–O(3)	1.13(3)
Os(2)–Os(1)–Os(3)	59.8(1)	Os(1)–Os(2)–Os(3)	60.0(1)
Os(1)–Os(3)–Os(2)	60.1(1)	Os(2)–Os(1)–C(11)	160.1(7)
Os(3)–Os(1)–C(11)	101.3(6)	Os(2)–Os(1)–C(12)	95.8(9)
Os(3)–Os(1)–C(12)	154.5(10)	Os(2)–Os(1)–C(13)	96.1(9)
Os(3)–Os(1)–C(13)	84.3(6)	C(11)–Os(1)–C(13)	87.3(12)
C(11)–Os(1)–C(12)	103.7(11)	C(12)–Os(1)–C(13)	91.6(11)
Os(2)–Os(1)–S(1)	87.4(2)	Os(3)–Os(1)–S(1)	95.9(1)
C(11)–Os(1)–S(1)	88.7(8)	C(12)–Os(1)–S(1)	89.9(9)
C(13)–Os(1)–S(1)	176.0(1)	Os(1)–Os(2)–C(21)	163.4(8)
Os(3)–Os(2)–C(21)	103.9(8)	Os(1)–Os(2)–C(22)	90.2(11)
Os(3)–Os(2)–C(22)	149.4(11)	C(21)–Os(2)–C(22)	106.2(14)
Os(1)–Os(2)–C(23)	84.9(11)	Os(3)–Os(2)–C(23)	95.1(11)
Os(1)–C(11)–O(11)	177.4(19)	Os(1)–C(12)–O(12)	176(3)
Os(1)–C(13)–O(13)	178(3)	Os(1)–S(1)–C(1)	110.5(9)
S(1)–C(1)–S(2)	140.5(16)	S(1)–C(1)–Fe	138.8(14)
S(2)–C(1)–Fe	80.7(9)	C(1)–S(2)–Fe	55.3(8)
S(2)–Fe–C(1)	43.9(7)	S(2)–Fe–C(2)	149.7(7)
S(2)–Fe–C(3)	108.9(7)	S(2)–Fe–P(1)	91.5(3)
S(2)–Fe–P(2)	91.5(3)	C(2)–Fe–C(3)	101.3(10)
C(2)–Fe–P(1)	88.9(9)	C(2)–Fe–P(2)	89.4(9)
C(3)–Fe–P(1)	88.5(8)	C(3)–Fe–P(2)	89.4(9)
P(1)–Fe–P(2)	176.8(3)		

**Fig. 3** The molecular structure of [(PEt₃)₂(CO)₂Fe(μ - η^2 : η^1 -CS₂)Os₃(CO)₁₁] **8a**

is confirmed, the bonding to the iron centre being unchanged and the second S atom of the disulfide bonding to an osmium atom in an axial position. The site preference of ligands depends on a balance of steric and electronic factors.^{18,19} Simple calculations on [Os₃(CO)₁₂–*n*L_{*n*}] systems show that the equatorial sites in approximately anticuboctahedral structures are less sterically hindered than axial sites.²⁰ It is therefore interesting that in **8a**, co-ordination occurs through an axial site on the osmium atom of the cluster especially since in the only other structurally characterised example of a triosmium cluster

containing a σ -co-ordinated sulfur moiety, $[\text{Os}_3(\text{CO})_{11}\{\text{S}(\text{CH}_2)_3\}]$,²¹ the ligand occupies the expected equatorial position. If the S was co-ordinated equatorially in **8b** there would be considerable steric repulsions between the carbonyl groups on the osmium cluster with those on the iron centre. Electronic arguments must also be taken into account. Both $[\text{Os}_3(\text{CO})_{11}(\text{MeCN})]$ and $[\text{Os}_3(\text{CO})_{10}(\text{MeCN})_2]$ exhibit axial co-ordination of the σ -donor ligands, this being due to the σ -donor characteristics of these ligands. Good σ -donor ligands, such as acetonitrile, prefer to lie *trans* to a carbonyl group rather than, in the case of good π -acceptor ligands, *trans* to the metal–metal bonds.²²

The Os–Os bonds are not significantly different to those in $[\text{Os}_3(\text{CO})_{12}]$ ²³ in contrast to the case of $[\text{Os}_3(\text{CO})_{11}\{\text{S}(\text{CH}_2)_3\}]$ ²¹ where the equatorially situated thietane group exerts a significant *trans* influence lengthening one of the metal–metal bonds. Unlike the case of **7b**, in **8a** the σ -co-ordinated sulfur atom does not seem to have any significant effect on the *trans* situated carbonyl group on Os(1). This may be explained by a delocalisation of the electron density across all the carbonyl bonds in the cluster rather than the localised effect seen in **7b**.

The photochemical reaction of $[\text{Fe}(\text{CO})_2(\text{PR}_3)_2(\eta^2\text{-CS}_2)]$ with $[\text{Os}_3(\text{CO})_{12}]$ is significantly lower for $\text{R} = \text{Ph}$ (**3a**) than for $\text{R} = \text{Et}$ (**3b**). In the case of the former, reaction is significantly slower and a significant quantity of $[\text{Os}_3(\text{CO})_{11}(\text{PPh}_3)]$ is formed as a by-product. Since a facile phosphine exchange has been observed for $[\text{Fe}(\text{CO})_2(\text{PR}_3)_2(\eta^2\text{-CS}_2)]$ ^{9,10} complexes and **3b** is particularly unstable in solution,⁸ dissociation of triphenylphosphine is not unexpected. The slower reaction of **3a** as compared to **3b** may be due to both the increased steric bulk²⁴ and decreased basicity²⁵ of PPh_3 as compared to PET_3 which both restricts access of **3b** to the available co-ordination site on the osmium cluster and results in a less nucleophilic donor sulfur atom in the PPh_3 -substituted compound.

The reaction chemistry of $[(\text{PET}_3)_2(\text{CO})_2\text{Fe}(\mu\text{-}\eta^2\text{:}\eta^1\text{-CS}_2)\text{M}(\text{CO})_5]$ ($\text{M} = \text{Cr}, \text{Mo}$ or W)

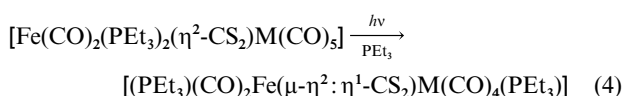
There are few CS_2 -containing compounds for which reactivity studies have been reported. These include $[\{\text{Pt}(\text{Ph}_2\text{PCH}_2\text{-PPh}_2)\text{Cl}\}_2(\mu\text{-CS}_2)]$ ²⁶ and $[\text{Pt}_2(\text{PBu}_2\text{Ph})_2(\mu\text{-CS}_2)]$ ^{27,28} which contain a dithiocarboxylate-type disulfide unit. In an attempt to compare the chemistry of the dithiocarboxylate and $\sigma + \pi$ bonding modes of carbon disulfide, some reaction chemistry of $[(\text{PET}_3)_2(\text{CO})_2\text{Fe}(\mu\text{-}\eta^2\text{:}\eta^1\text{-CS}_2)\text{M}(\text{CO})_5]$ ($\text{M} = \text{Cr}$ **5a**, Mo **6a** or W **7a**) has been investigated. Since one approach to building organometallic clusters involves the interaction of a metal fragment with the CS_2 moiety of a co-ordinated disulfide complex inducing fragmentation of CS_2 to yield S and CS ligands, attempts at cluster synthesis have been made here. There are only a few examples of clusters reported in the literature as a result of this type of fragmentation of CS_2 ; these include $[(\text{CoCp})_3(\mu_3\text{-CS})(\mu\text{-S})]$ ($\text{Cp} = \eta^5\text{-C}_5\text{H}_5$)²⁹ and $[\text{Fe}_4(\text{CO})_{12}(\mu_3\text{-CS})(\mu\text{-S})]$.³⁰

No reaction was observed between $[(\text{PET}_3)_2(\text{CO})_2\text{Fe}(\mu\text{-}\eta^2\text{:}\eta^1\text{-CS}_2)\text{M}(\text{CO})_5]$ (**5a–7a**) and $[\text{N}(\text{PPh}_3)_2][\text{BF}_4]$ or NEt_3 using either 1 equivalent or a significant excess of the reagents. There was also no observed reaction between **5a**, **6a** or **7a** and ammonia at either room temperature or at elevated temperatures. This suggests that these complexes are not susceptible to nucleophilic attack either at the CS_2 moiety or at the Group 6 metal centre. This parallels the reaction chemistry of $[\text{Pt}_2(\text{PBu}_2\text{Ph})_2(\mu\text{-CS}_2)]$.³⁰ This is in agreement with the proposal¹⁴ that the CS_2 ligand must bridge a metal–metal bond before fragmentation can occur.

Broad-band UV photolysis of a thf solution of **5a**, **6a** or **7a** with PET_3 leads to substitution of the Group 6 metal centre yielding $[(\text{PET}_3)_2(\text{CO})_2\text{Fe}(\mu\text{-}\eta^2\text{:}\eta^1\text{-CS}_2)\text{M}(\text{CO})_4(\text{PET}_3)]$ ($\text{M} = \text{Cr}$ **9a**, Mo **10a**, W **11a**) [equation (4)] as characterised initially by

Table 3 Selected bond lengths and angles for complex **9a**

Fe–S(1)	2.342(1)	Fe–C(1)	1.934(3)
Fe–P(1)	2.276(1)	Fe–P(2)	2.273(1)
Fe–C(14)	1.796(4)	Fe–C(15)	1.755(4)
S(1)–C(1)	1.674(3)	C(1)–S(2)	1.639(3)
S(2)–Cr	2.431(1)	P(1)–C(2)	1.805(5)
P(1)–C(4)	1.840(6)	P(1)–C(6)	1.801(4)
C(2)–C(3)	1.514(8)	C(4)–C(5)	1.496(7)
C(6)–C(7)	1.536(8)	P(2)–C(8)	1.839(5)
P(2)–C(10)	1.837(3)	P(2)–C(12)	1.829(4)
C(14)–O(1)	1.138(5)	C(15)–O(2)	1.142(5)
Cr–P(3)	2.398(1)	Cr–C(22)	1.823(4)
Cr–C(23)	1.850(4)	Cr–C(24)	1.884(3)
Cr–C(25)	1.885(4)	P(3)–C(16)	1.850(4)
P(3)–C(18)	1.852(3)	P(3)–C(20)	1.829(5)
C(16)–C(17)	1.519(5)	C(18)–C(19)	1.521(5)
C(20)–C(21)	1.539(7)	C(22)–O(3)	1.160(5)
C(23)–O(4)	1.158(5)	C(24)–O(5)	1.149(4)
C(25)–O(6)	1.139(5)		
S(1)–Fe–C(1)	44.8(1)	S(1)–Fe–P(1)	93.0(1)
S(1)–Fe–P(2)	89.0(1)	S(1)–Fe–C(14)	115.1(1)
S(1)–Fe–C(15)	141.9(1)	C(1)–Fe–P(1)	93.2(1)
C(1)–Fe–P(2)	91.7(1)	C(1)–Fe–C(14)	160.0(2)
C(1)–Fe–C(15)	96.2(2)	P(1)–Fe–P(2)	174.7(1)
P(1)–Fe–C(14)	86.9(1)	P(1)–Fe–C(15)	90.2(1)
P(2)–Fe–C(14)	87.9(1)	P(2)–Fe–C(15)	91.4(1)
C(14)–Fe–C(15)	103.8(2)	Fe–S(1)–C(1)	54.6(1)
Fe–C(1)–S(1)	80.6(1)	Fe–C(1)–S(2)	139.7(2)
S(1)–C(1)–S(2)	139.7(2)	C(1)–S(1)–Cr	120.3(1)
Fe–C(14)–O(1)	177.2(3)	Fe–C(15)–O(2)	175.9(4)
S(2)–Cr–P(3)	92.9(1)	S(2)–Cr–C(22)	172.2(2)
S(2)–Cr–C(23)	88.5(1)	S(2)–Cr–C(24)	96.2(1)
S(2)–Cr–C(25)	87.5(1)	P(3)–Cr–C(22)	93.5(1)
P(3)–Cr–C(23)	179.1(1)	P(3)–Cr–C(24)	90.0(1)
P(3)–Cr–C(25)	89.7(1)	C(22)–Cr–C(23)	85.9(2)
C(22)–Cr–C(24)	89.0(2)	C(22)–Cr–C(25)	87.3(2)
C(23)–Cr–C(24)	89.3(2)	C(23)–Cr–C(25)	90.9(2)
C(24)–Cr–C(25)	176.3(2)	Cr–C(22)–O(3)	176.3(4)
Cr–C(23)–O(4)	176.3(3)	Cr–C(24)–O(5)	174.8(3)
Cr–C(25)–O(6)	175.0(3)		



IR and ^1H NMR spectroscopy. Vibrational analysis of the IR spectra points towards a *cis* disposition of the phosphine and CS_2 ligands at the Group 6 metal centre. It is presumed that the reaction occurs by way of a simple attack of PET_3 on $[(\text{PET}_3)_2(\text{CO})_2\text{Fe}(\mu\text{-}\eta^2\text{:}\eta^1\text{-CS}_2)\text{M}(\text{CO})_4(\text{thf})]$, the latter formed by photosubstitution of a carbonyl group by thf. Definitive characterisation of $[(\text{PET}_3)_2(\text{CO})_2\text{Fe}(\mu\text{-}\eta^2\text{:}\eta^1\text{-CS}_2)\text{Cr}(\text{CO})_4(\text{PET}_3)]$ **9a** was made by a single-crystal X-ray diffraction study (Fig. 4). Selected bond lengths and angles are given in Table 3.

The bonding around the iron centre in **9a** is unaffected by the phosphine substitution at chromium. As in **7b** and **8a**, the disulfide unit forms a π bond to iron and a σ bond to the Group 6 metal. The C(1)–S(1) and C(1)–S(2) bond lengths are not significantly different at the 3σ level. By extending the currently accepted theory for bonding of CS_2 to transition metals,⁸ a possible explanation for the similarity in C(1)–S(1) and C(1)–S(2) bond lengths may be forwarded. The good π -accepting properties of the π -co-ordinating CS_2 ligand are explained in terms of three modes of interaction. Initially the π^* orbitals on the π -co-ordinated C–S bond accept electron density from the metal centre. This is augmented by π acceptance by the d orbitals of the co-ordinated sulfur from the metal in a $d_\pi\text{--}d_\pi$ interaction and by π^* orbitals of the unco-ordinated C–S bond which lies perpendicular to the *xy* plane and is able to accept electron density from the filled d_{xz} and d_{yz} orbitals on the metal. These three interactions result in lengthening of both the C–S co-ordinated and C–S unco-ordinated bonds as is seen in

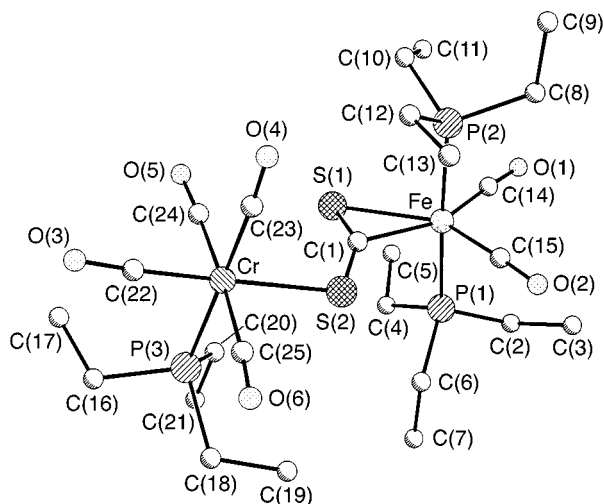


Fig. 4 The molecular structure of $[(\text{PEt}_3)_2(\text{CO})_2\text{Fe}(\mu\text{-}\eta^2\text{:}\eta^1\text{-CS}_2)\text{-Cr}(\text{CO})_4(\text{PEt}_3)]$ **9a**

$[\text{Fe}(\text{CO})_2(\text{PMe}_3)(\text{PPh}_3)(\eta^2\text{-CS}_2)]$,¹⁰ where the bond lengths for co-ordinated and unco-ordinated C–S bonds are 1.676 and 1.615 Å, respectively (*cf.* C–S bond length of 1.56 Å in free CS_2 ³¹). On donation from the unco-ordinated sulfur, as seen in **3a**, to osmium, as seen in **8a**, back-donation from the iron centre to the π^* orbitals of the C–S bond to osmium is increased and that to the π^* set of the C–S bond to iron decreased. Overall this gives an increase in the electron density donated to the orbitals related to the C–S bond to osmium and hence a lengthening of that bond, this equating the two C–S bond lengths. Alternatively, there may be some donation from filled non-bonding orbitals on the sulfur co-ordinated to the iron to the π^* orbitals of the C–S bond to osmium. This would increase the strength of the bond co-ordinated to iron and decrease that of the other.

This confirms the postulation made for **8a** that donation from the unco-ordinated sulfur of a π CS_2 ligand to a metal centre surrounded by good π -acceptor ligands removes electron density from the sulfur leaving it relatively δ^+ . This leads to an electron drift towards that sulfur from the carbon of the disulfide unit. To compensate for this either back donation from iron to π^* orbitals of the C(1)–S(1) bond is reduced or electron density is donated from the filled non-bonding orbitals S(1) to C(1). This increases the carbene character of the Fe(1)–C(1) bond; this being less marked in **9a** [Fe(1)–C(1) = 1.934(3) Å] as compared to **8a**.

Of interest is the *cis* disposition of the CS_2 and PEt_3 ligands at the Cr centre in **9a**. Steric arguments would favour a *trans* arrangement as is observed in all the crystallographically characterised $\text{S-Cr}(\text{CO})_4\text{-P}$ fragments published to date³² with the exception of those with a bidentate S–P containing ligand where *cis* geometry is forced. However, the *cis* disposition of the S and P ligands about the metal centre has the advantage that these σ -donor ligands are then both *trans* to π -accepting carbonyls. This has a co-operative effect, the strength of the M–S and M–P bonds being increased as does that of the *trans* situated carbonyl groups.

The phosphine-substituted complexes $[(\text{PEt}_3)_2(\text{CO})_2\text{Fe}(\mu\text{-}\eta^2\text{:}\eta^1\text{-CS}_2)\text{M}(\text{CO})_4(\text{PEt}_3)]$ can also be prepared thermally. In refluxing methanol, $[(\text{PEt}_3)_2(\text{CO})_2\text{Fe}(\mu\text{-}\eta^2\text{:}\eta^1\text{-CS}_2)\text{M}(\text{CO})_5]$ reacts with PEt_3 to give moderate yields of $[(\text{PEt}_3)_2(\text{CO})_2\text{Fe}(\mu\text{-}\eta^2\text{:}\eta^1\text{-CS}_2)\text{M}(\text{CO})_4(\text{PEt}_3)]$ (**9a** or **10b**) together with $[\text{Fe}(\text{CO})_2(\text{PEt}_3)_2(\eta^2\text{-CS}_2)]$ **3a**. The reaction times varied from 2½ h for Cr to 54 h for W, this being a measure of the relative kinetic stability of the reactants. For thermolysis, like photolysis, the reaction must be performed in a co-ordinating solvent; reaction in refluxing hexane leads to decomposition. This is a situation where photolysis is the synthetic method of

choice for substitution since yields are higher and reaction times shorter. This gives credence to our assertion that photochemistry not only offers a route to novel complexes but also to known products both faster and in higher yields than the analogous thermolytic pathways.

Conclusion

Photochemistry has been used to generate a number of hetero-bimetallic complexes containing $\pi + \sigma$ CS_2 bridging groups. Unlike thermolysis reactions in which often the CS_2 moiety is broken, in the case of photolysis the CS_2 unit remains intact. Broad-band UV photolysis of thf solutions of $[\text{M}(\text{CO})_6]$ ($\text{M} = \text{Cr}, \text{Mo}$ or W) and acetonitrile solutions of $[\text{Os}_3(\text{CO})_{12}]$ with $[\text{Fe}(\text{CO})_2(\text{PR}_3)_2(\eta^2\text{-CS}_2)]$ ($\text{R} = \text{Et}$ **3a** or Ph **3b**) leads to the formation of the bimetallic complexes $[(\text{PR}_3)_2(\text{CO})_2\text{Fe}(\mu\text{-}\eta^2\text{:}\eta^1\text{-CS}_2)\text{M}(\text{CO})_5]$ ($\text{R} = \text{Et}$, $\text{M} = \text{Cr}$ **5a**, Mo **6a** or W **7a**; $\text{R} = \text{Ph}$, $\text{M} = \text{Cr}$ **5b**, Mo **6b** or W **7b**) and $[(\text{PR}_3)_2(\text{CO})_2\text{Fe}(\mu\text{-}\eta^2\text{:}\eta^1\text{-CS}_2)\text{Os}_3(\text{CO})_{11}]$ ($\text{R} = \text{Et}$ **3a** or Ph **3b**) respectively. The reaction chemistry of $[(\text{PEt}_3)_2(\text{CO})_2\text{Fe}(\mu\text{-}\eta^2\text{:}\eta^1\text{-CS}_2)\text{M}(\text{CO})_5]$ (**5a–7a**) has been investigated and it is found that these complexes are not susceptible to nucleophilic attack either at the CS_2 moiety or at the Group 6 metal centre. Broad-band UV photolysis of a thf solution of $[(\text{PEt}_3)_2(\text{CO})_2\text{Fe}(\mu\text{-}\eta^2\text{:}\eta^1\text{-CS}_2)\text{M}(\text{CO})_5]$ (**5a–7a**) with PEt_3 leads to the formation of the phosphine-substituted complexes $[(\text{PPh}_3)_2(\text{CO})_2\text{Fe}(\mu\text{-}\eta^2\text{:}\eta^1\text{-CS}_2)\text{M}(\text{CO})_4(\text{PEt}_3)]$ ($\text{M} = \text{Cr}$ **9a** or Mo **10b**).

Experimental

General

Unless stated otherwise, all syntheses were performed under an inert atmosphere of dry nitrogen using standard Schlenk techniques. All photochemical reactions were performed in a specially designed glass reaction vessel fitted with a nitrogen bubbler, reflux condenser and dry-ice cooling finger. A 125 W mercury arc broad-band UV lamp was used as the irradiation source and reflectors placed around the reaction vessel to maximise efficiency. The reaction mixtures were maintained at low temperature by means of a dry-ice cooling finger. Routine separation of products was performed by thin-layer chromatography (TLC), using commercially prepared glass plates, pre-coated to a thickness of 0.25 mm with Merck Kieselgel 60 F_{254} as supplied by Merck. Alternatively laboratory prepared glass plates, coated to a thickness of 1.0 mm with Merck Kieselgel 60 F_{254} , were used. All reagents were purchased from commercial sources and used as received unless noted otherwise. Literature methods were used to prepare $[\text{Os}_3(\text{CO})_{12}]$.³³

Physical measurements

Infrared spectra were recorded using a Perkin-Elmer PE 1710 Fourier-transform infrared spectrometer, solution spectra in NaCl solution cells (path length 0.5 mm) and solid-state spectra in compressed KBr pellets. All values quoted are in wavenumbers (cm^{-1}). The ^1H NMR spectra were recorded using Bruker AM400, WM250 or WP80SY Fourier-transform NMR spectrometers and data reported using the chemical shift scale in units of ppm relative to the solvent resonance. Fast atom bombardment (FAB) mass spectra were recorded using a KRATOS MS-50 spectrometer, with either 3-nitrobenzyl alcohol or thioglycerol as a matrix and CsI as calibrant. Microanalyses were performed by the Department of Chemistry microanalysis section. Infrared and NMR data are collected in Table 4 and yields, mass spectral and microanalytical data in Table 5.

Photolyses

[Fe(CO)₅] 1 with CS₂ in thf. A thf solution of $[\text{Fe}(\text{CO})_5]$ **1**

Table 4 Infrared and NMR data for the carbon disulfide complexes

Compound	$\nu(\text{CO})^a/\text{cm}^{-1}$	$\nu(\text{CS})^b/\text{cm}^{-1}$	$\delta(^1\text{H})^c$
3a $[\text{Fe}(\text{CO})_2(\text{PET}_3)_2(\eta^2\text{-CS}_2)]$	1982s, 1921vs	1116	1.60 (m, CH_2), 1.18 (m, CH_3)
3b $[\text{Fe}(\text{CO})_2(\text{PPh}_3)_2(\eta^2\text{-CS}_2)]$	1992s, 1932vs	1143	7.55 (m, Ph)
4a $[\text{Fe}(\text{CO})_2(\text{PET}_3)_2(\eta^2\text{-CS}_2\text{Me})]^+$	2035s, 1973vs	1140	3.13 (s, SCH_3), 1.64 (m, CH_2), 1.12 (m, CH_3)
5a $[(\text{PET}_3)_2(\text{CO})_2\text{Fe}(\mu\text{-}\eta^2\text{:}\eta^1\text{-CS}_2)\text{Cr}(\text{CO})_5]$	2054m, 1996s, 1982s, 1934 (sh), 1926vs, 1879m	1132	1.67 (m, CH_2), 1.21 (m, CH_3)
6a $[(\text{PET}_3)_2(\text{CO})_2\text{Fe}(\mu\text{-}\eta^2\text{:}\eta^1\text{-CS}_2)\text{Mo}(\text{CO})_5]$	2064m, 1996s, 1981s, 1933 (sh), 1928vs, 1885m	1131	1.70 (m, CH_2), 1.18 (m, CH_3)
7a $[(\text{PET}_3)_2(\text{CO})_2\text{Fe}(\mu\text{-}\eta^2\text{:}\eta^1\text{-CS}_2)\text{W}(\text{CO})_5]$	2062m, 1999s, 1983s, 1935 (sh), 1920vs, 1880m	1111	1.68 (m, CH_2), 1.19 (m, CH_3)
5b $[(\text{PPh}_3)_2(\text{CO})_2\text{Fe}(\mu\text{-}\eta^2\text{:}\eta^1\text{-CS}_2)\text{Cr}(\text{CO})_5]$	2055m, 2002m, 1982s, 1940 (sh), 1928s, 1884s	^d	7.45 (m, Ph)
6b $[(\text{PPh}_3)_2(\text{CO})_2\text{Fe}(\mu\text{-}\eta^2\text{:}\eta^1\text{-CS}_2)\text{Mo}(\text{CO})_5]$	2069m, 2005m, 1984s, 1948 (sh), 1923s, 1884s	^d	7.60 (m, Ph)
7b $[(\text{PPh}_3)_2(\text{CO})_2\text{Fe}(\mu\text{-}\eta^2\text{:}\eta^1\text{-CS}_2)\text{W}(\text{CO})_5]$	2064m, 2004m, 1986s, 1943 (sh), 1926s, 1887s	1141	7.45 (m, Ph)
8a $[(\text{PET}_3)_2(\text{CO})_2\text{Fe}(\mu\text{-}\eta^2\text{:}\eta^1\text{-CS}_2)\text{Os}_3(\text{CO})_{11}]$	2098w, 2045s, 2027m, 2009s, 1998 (sh), 1986w, 1977m, 1964w, 1949m	1099	1.77 (m, CH_2), 1.18 (m, CH_3)
8b $[(\text{PPh}_3)_2(\text{CO})_2\text{Fe}(\mu\text{-}\eta^2\text{:}\eta^1\text{-CS}_2)\text{Os}_3(\text{CO})_{11}]$	2098w, 2044s, 2023m, 2008s, 2002 (sh), 1974w, 1964m, 1940m	1129	7.47 (m, Ph)
9a $[(\text{PET}_3)_2(\text{CO})_2\text{Fe}(\mu\text{-}\eta^2\text{:}\eta^1\text{-CS}_2)\text{Cr}(\text{CO})_4(\text{PET}_3)]$	2003 (sh), 2000w, 1990s, 1934m, 1900m, 1889s, 1864s	^d	1.72 (m, CH_2), 1.12 (m, CH_3)
10a $[(\text{PET}_3)_2(\text{CO})_2\text{Fe}(\mu\text{-}\eta^2\text{:}\eta^1\text{-CS}_2)\text{Mo}(\text{CO})_4(\text{PET}_3)]$	2010 (sh), 2008w, 1991s, 1924m, 1900m, 1889s, 1865s	^d	1.69 (m, CH_2), 1.15 (m, CH_3)
11a $[(\text{PET}_3)_2(\text{CO})_2\text{Fe}(\mu\text{-}\eta^2\text{:}\eta^1\text{-CS}_2)\text{W}(\text{CO})_4(\text{PET}_3)]$	2010 (sh), 2005w, 1990s, 1934s, 1897m, 1886s, 1861s	^d	1.70 (m, CH_2), 1.09 (m, CH_3)

^a Hexane solution. ^b Nujol mull. ^c In CDCl_3 . ^d Not unambiguously assigned.**Table 5** Yields, mass spectral and microanalytical data for the carbon disulfide complexes

Compound	Yield (%)	m/z	Analyses ^a (%)			
			C	H	P	S
3a $[\text{Fe}(\text{CO})_2(\text{PET}_3)_2(\eta^2\text{-CS}_2)]$	80	424	—	—	—	—
3b $[\text{Fe}(\text{CO})_2(\text{PPh}_3)_2(\eta^2\text{-CS}_2)]$	75	712	—	—	—	—
4a $[\text{Fe}(\text{CO})_2(\text{PET}_3)_2(\eta^2\text{-CS}_2)]^+$	95	—	—	—	—	—
5a $[(\text{PET}_3)_2(\text{CO})_2\text{Fe}(\mu\text{-}\eta^2\text{:}\eta^1\text{-CS}_2)\text{Cr}(\text{CO})_5]$	65	616	39.17 (38.97)	4.97 (4.91)	10.32 (10.05)	10.09 (10.40)
6a $[(\text{PET}_3)_2(\text{CO})_2\text{Fe}(\mu\text{-}\eta^2\text{:}\eta^1\text{-CS}_2)\text{Mo}(\text{CO})_5]$	60	622	36.61 (36.38)	4.75 (4.58)	9.22 (9.38)	10.91 (9.71)
7a $[(\text{PET}_3)_2(\text{CO})_2\text{Fe}(\mu\text{-}\eta^2\text{:}\eta^1\text{-CS}_2)\text{W}(\text{CO})_5]$	50	750	31.91 (32.11)	4.06 (4.04)	8.39 (8.28)	8.51 (8.57)
5b $[(\text{PPh}_3)_2(\text{CO})_2\text{Fe}(\mu\text{-}\eta^2\text{:}\eta^1\text{-CS}_2)\text{Cr}(\text{CO})_5]$	60	<i>b</i>	59.10 (58.42)	3.41 (3.34)	6.14 (6.85)	7.62 (7.09)
6b $[(\text{PPh}_3)_2(\text{CO})_2\text{Fe}(\mu\text{-}\eta^2\text{:}\eta^1\text{-CS}_2)\text{Mo}(\text{CO})_5]$	50	<i>b</i>	56.47 (55.71)	3.42 (3.19)	6.59 (6.53)	6.94 (6.76)
7b $[(\text{PPh}_3)_2(\text{CO})_2\text{Fe}(\mu\text{-}\eta^2\text{:}\eta^1\text{-CS}_2)\text{W}(\text{CO})_5]$	50	<i>b</i>	51.05 (50.99)	2.87 (2.92)	6.07 (5.98)	5.63 (6.19)
8a $[(\text{PET}_3)_2(\text{CO})_2\text{Fe}(\mu\text{-}\eta^2\text{:}\eta^1\text{-CS}_2)\text{Os}_3(\text{CO})_{11}]$	80	<i>b</i>	22.91 (23.97)	2.40 (2.32)	4.56 (4.75)	4.48 (4.92)
8b $[(\text{PPh}_3)_2(\text{CO})_2\text{Fe}(\mu\text{-}\eta^2\text{:}\eta^1\text{-CS}_2)\text{Os}_3(\text{CO})_{11}]$	50	<i>b</i>	38.05 (37.74)	2.07 (1.90)	3.95 (3.89)	4.06 (4.03)
9a $[(\text{PET}_3)_2(\text{CO})_2\text{Fe}(\mu\text{-}\eta^2\text{:}\eta^1\text{-CS}_2)\text{Cr}(\text{CO})_4(\text{PET}_3)]$	60 ^c /18 ^d	<i>b</i>				
10a $[(\text{PET}_3)_2(\text{CO})_2\text{Fe}(\mu\text{-}\eta^2\text{:}\eta^1\text{-CS}_2)\text{Mo}(\text{CO})_4(\text{PET}_3)]$	50 ^c /21 ^d	<i>b</i>				
11a $[(\text{PET}_3)_2(\text{CO})_2\text{Fe}(\mu\text{-}\eta^2\text{:}\eta^1\text{-CS}_2)\text{W}(\text{CO})_4(\text{PET}_3)]$	40 ^c /10 ^d	<i>b</i>				

^a Calculated values in parentheses. ^b Decomposes in mass spectrometer. ^c Photochemical. ^d Thermochemical.

(1 ml in 150 ml) containing excess CS_2 (1 ml) was irradiated using the broad-band UV source, the reaction mixture maintained at low temperature by means of the dry-ice cooling finger. A brown precipitate was formed, this being insoluble in common organic solvents and consequently characterisation of the photolysis products was not possible.

$[\text{Fe}(\text{CO})_3(\text{PR}_3)_2]$ (R = Et **2a or Ph **2b**) with CS_2 in dichloromethane.** In a typical reaction, a dichloromethane solution of $[\text{Fe}(\text{CO})_3(\text{PR}_3)_2]$ (R = Et **2a** or Ph **2b**) (30 mg in 150 ml) containing excess CS_2 (1 ml) was irradiated (3 h) using the broad-band UV source. From comparison with literature data⁷ it was proposed that the yellow complex $[\text{Fe}(\text{CO})_3(\text{PR}_3)_2(\eta^2\text{-CS}_2)]$ (R = Et **3a** or Ph **3b**) was formed. The product was purified by TLC (diethyl ether–hexane, 20:80, as eluent).

$[\text{Fe}(\text{CO})_3(\text{PET}_3)_2(\eta^2\text{-CS}_2)]$ **3a with methyl iodide in dichloromethane.** A dichloromethane solution of $[\text{Fe}(\text{CO})_3(\text{PET}_3)_2(\text{CS}_2)]$ (30 mg in 100 ml) was stirred with methyl iodide (1 ml) at room temperature for 2 h. The product $[\text{Fe}(\text{CO})_3(\text{PET}_3)_2(\eta^2\text{-CS}_2\text{Me})]^+$ was obtained as an orange crystalline material on addition of hexane.

$[\text{M}(\text{CO})_6]$ (M = Cr, Mo or W) with $[\text{Fe}(\text{CO})_3(\text{PR}_3)_2(\eta^2\text{-CS}_2)]$ (R = Me **3a or Ph **3b**) in thf.** In a typical reaction, a thf solution

of $[\text{M}(\text{CO})_6]$ (30 mg in 150 ml) containing a stoichiometric equivalent of $[\text{Fe}(\text{CO})_3(\text{PR}_3)_2(\eta^2\text{-CS}_2)]$ (**3a** or **3b**) was irradiated (4 h) using the broad-band UV source. From analysis of the spectral data it was proposed that the yellow complex $[(\text{PR}_3)_2(\text{CO})_2\text{Fe}(\mu\text{-}\eta^2\text{:}\eta^1\text{-CS}_2)\text{M}(\text{CO})_5]$ was formed. The product was purified by TLC (diethyl ether–hexane, 15:85, as eluent).

$[\text{Os}_3(\text{CO})_{12}]$ with $[\text{Fe}(\text{CO})_3(\text{PR}_3)_2(\eta^2\text{-CS}_2)]$ (R = Me **3a or Ph **3b**) in acetonitrile.** In a typical reaction, an acetonitrile solution of $[\text{Os}_3(\text{CO})_{12}]$ (40 mg in 150 ml) containing a stoichiometric equivalent of $[\text{Fe}(\text{CO})_3(\text{PR}_3)_2(\eta^2\text{-CS}_2)]$ (**3a** or **3b**) was irradiated (4 h) using the broad-band UV source. From analysis of the spectral data it was proposed that the dark red complex $[(\text{PR}_3)_2(\text{CO})_2\text{Fe}(\mu\text{-}\eta^2\text{:}\eta^1\text{-CS}_2)\text{Os}_3(\text{CO})_{11}]$ (**8a** or **8b**) was formed. The product was purified by TLC (dichloromethane–hexane, 20:80, as eluent).

$[(\text{PET}_3)_2(\text{CO})_2\text{Fe}(\mu\text{-}\eta^2\text{:}\eta^1\text{-CS}_2)\text{M}(\text{CO})_5]$ (M = Cr **5a, Mo **6a** or W **7a**) with PET_3 in thf.** A thf solution of $[(\text{PET}_3)_2(\text{CO})_2\text{Fe}(\mu\text{-}\eta^2\text{:}\eta^1\text{-CS}_2)\text{M}(\text{CO})_5]$ (**5a**, **6a** or **7a**) (30 mg in 150 ml) containing excess PET_3 (1 ml) was irradiated (2 h) using the broad-band UV source. From analysis of the spectral data it was proposed that the orange complex $[(\text{PET}_3)_2(\text{CO})_2\text{Fe}(\mu\text{-}\eta^2\text{:}\eta^1\text{-CS}_2)\text{M}(\text{CO})_4(\text{PET}_3)]$ was formed. The product was purified by TLC (diethyl ether–hexane, 20:80, as eluent).

Table 6 Crystal data and structure refinement parameters for $[(\text{PPh}_3)_2(\text{CO})_2\text{Fe}(\mu\text{-}\eta^2\text{:}\eta^1\text{-CS}_2)\text{W}(\text{CO})_5]$ **7b**, $[(\text{PEt}_3)_2(\text{CO})_2\text{Fe}(\mu\text{-}\eta^2\text{:}\eta^1\text{-CS}_2)\text{Os}_3(\text{CO})_{11}]$ **8a** and $[(\text{PEt}_3)_2(\text{CO})_2\text{Fe}(\mu\text{-}\eta^2\text{:}\eta^1\text{-CS}_2)\text{Cr}(\text{CO})_4(\text{PEt}_3)]$ **9a**^a

Compound	7b	8a	9a
Molecular formula	$\text{C}_{44}\text{H}_{30}\text{FeO}_7\text{P}_2\text{S}_2\text{W}$	$\text{C}_{26}\text{H}_{30}\text{FeO}_{13}\text{Os}_3\text{P}_2\text{S}_2$	$\text{C}_{25}\text{H}_{45}\text{CrFeO}_6\text{P}_3\text{S}_2$
<i>M</i>	1036.62	1304.23	704.45
Crystal habit	Yellow needles	Dark brown needles	Orange blocks
Crystal size/mm	$0.38 \times 0.19 \times 0.11$	$0.23 \times 0.16 \times 0.14$	$0.27 \times 0.24 \times 0.23$
<i>a</i> /Å	12.024(3)	10.496(3)	8.522(3)
<i>b</i> /Å	13.029(4)	13.532(4)	12.320(4)
<i>c</i> /Å	16.412(5)	14.625(5)	18.386(6)
α /°	101.47(3)	89.19(3)	102.09(3)
β /°	103.46(3)	74.11(3)	99.88(3)
γ /°	115.70(3)	72.55(3)	106.53(3)
<i>U</i> /Å ³	2117	1901	1754
<i>Z</i>	2	2	2
<i>D_c</i> /Mg m ⁻³	1.626	2.278	1.334
<i>F</i> (000)	1024	1212	740
μ /mm ⁻¹	3.297	10.590	0.962
Maximum, minimum transmission	0.948, 0.779	0.931, 0.451	0.577, 0.551
Index ranges	$-14 \leq h \leq 14$, $-16 \leq k \leq 16$, $0 \leq l \leq 20$	$-10 \leq h \leq 11$, $-16 \leq k \leq 17$, $0 \leq l \leq 18$	$-8 \leq h \leq 8$, $-15 \leq k \leq 15$, $0 \leq l \leq 23$
Reflections measured	4687	3354	4825
Independent reflections (<i>R</i> _{int})	4175 (0.0167)	3015 (0.0076)	4138 (0.0054)
Parameters, restraints	257, 8	299, 0	344, 0
<i>R</i> 1 ^b	0.0590	0.0512	0.0337
<i>wR</i> 1 ^b	0.0589	0.0467	0.0347
<i>P</i> ^b	0.001	0.000	0.0003
Observed reflections	3769 [<i>F</i> > 4σ(<i>F</i>)]	2436 [<i>F</i> > 4σ(<i>F</i>)]	4059 [<i>F</i> > 3σ(<i>F</i>)]
Peak, hole in final difference map/e Å ⁻³	1.890, -1.836	1.529, -1.151	0.624, -0.337

^a Details in common: crystal system triclinic; space group *P* $\bar{1}$ (no. 2); data collection range $3.0 < 2\theta < 55.0^\circ$. ^b $R1 = \sum ||F_o| - |F_c|| / \sum |F_o|$, $wR1 = [\sum w^2(|F_o| - |F_c|)^2 / \sum w^2 F_o^2]^{1/2}$, $w = 1/[\sigma^2(F_o)^2 + P F^2]$.

X-Ray crystallography

Structural determinations were undertaken on single crystals of $[(\text{PPh}_3)_2(\text{CO})_2\text{Fe}(\mu\text{-}\eta^2\text{:}\eta^1\text{-CS}_2)\text{W}(\text{CO})_5]$ **7b**, $[(\text{PEt}_3)_2(\text{CO})_2\text{Fe}(\mu\text{-}\eta^2\text{:}\eta^1\text{-CS}_2)\text{Os}_3(\text{CO})_{11}]$ **8a** and $[(\text{PEt}_3)_2(\text{CO})_2\text{Fe}(\mu\text{-}\eta^2\text{:}\eta^1\text{-CS}_2)\text{Cr}(\text{CO})_4(\text{PEt}_3)]$ **9a** using X-ray diffraction analyses. All measurements were made at 298 K with graphite-monochromated radiation ($\lambda = 0.71073$ Å) in the ω - θ scan mode on a Stoe-Siemens AED diffractometer. Crystal data and data acquisition details are summarised in Table 6. Cell parameters were obtained by least-squares refinement on diffractometer angles from 25 centred reflections ($20 < 2\theta < 22.5^\circ$). Semiempirical absorption corrections based on ψ -scan data were applied for **7b**, **8a** and **9a**.³⁴

The structures were solved by direct (**8a** and **9a**) and Patterson methods (**7b**) followed by Fourier-difference syntheses and refined by blocked-cascade (**8a** and **9a**) or full-matrix (**7b**) least-squares fits on *F* (SHELXL 76).³⁵ All non-hydrogen atoms in **9a**, W, Fe, P, S, and C and O atoms of ordered CO ligands in **7b** and Os, Fe, P, S, and C and O atoms of CO ligands on Fe and some C atoms of Et groups in **8a** were treated anisotropically. Some of the ethyl groups in **8a** were subject to slight thermal libration which could not be described successfully with a two-fold disorder model. The hydrogen atoms were placed in idealised positions and allowed to ride on the relevant carbon atom. In the final cycles of refinement a weighting scheme was introduced which produced a flat analysis of variance. The phenyl rings on the triphenylphosphine moieties in **7b** were refined as rigid groups. The CS₂ group and one of the carbonyl groups in **7b** are disordered over two orientations about the C(1)–S(1) and C(22)–O(22) bonds with relative occupancies 0.67 and 0.33 and were refined isotropically with restraints to the Fe–S(1), Fe–S(1'), Fe–C(1), Fe–C(1'), C(1)–S(2), C(1')–S(2'), Fe–C(22') and C(22')–O(22') distances and thermal parameters of atoms S(1), S(1'), C(1), C(1'), C(22), O(22), C(22'), O(22'). Those atoms of the minor contribution are annotated with a prime ('). As a further check, alternative settings of the cell were checked for the presence of a twin, but no reasonable alternatives could be found. The final

difference syntheses revealed two peaks of weight ≥ 1 e Å⁻³ at distances of *ca.* 1 Å from W in **7b**, these and similar peaks in the vicinity of the Os atoms in **8a** have no chemical significance and may be ascribed to absorption effects.

CCDC reference number 186/744.

Acknowledgements

Girton College Cambridge is thanked for a Research Fellowship. This work was funded in part by the EPSRC. The advice and assistance of G. P. Shields and R. E. Hosking is greatly appreciated.

References

- (a) J.-P. Collin and J.-P. Sauvage, *Coord. Chem. Rev.*, 1989, **93**, 245; (b) J. Ibers, *Chem. Soc. Rev.*, 1982, **43**, 165.
- K. K. Pandey, *Coord. Chem. Rev.*, 1995, **140**, 37.
- B. C. Gates, J. R. Katzer and G. C. A. Schmit, *The Chemistry of Catalytic Processes*, McGraw-Hill, New York, 1979.
- P. V. Broadhurst, B. F. G. Johnson, J. Lewis and P. R. Raithby, *J. Chem. Soc., Chem. Commun.*, 1982, 140.
- For examples, see, N. E. Leadbeater, *J. Chem. Soc., Dalton Trans.*, 1995, 2923.
- A. J. Edwards, N. E. Leadbeater, J. Lewis and P. R. Raithby, *J. Organomet. Chem.*, 1995, **512**, 13.
- M. Rosi, A. Sgmellotti, F. Tarantelli and C. Floriani, *J. Organomet. Chem.*, 1987, **332**, 153.
- M. C. Baird, G. Hartwell and G. Wilkinson, *J. Chem. Soc. A*, 1967, 2037.
- P. Conway, S. M. Grant and A. R. Manning, *J. Chem. Soc., Dalton Trans.*, 1979, 1920.
- H. Le Bozec, P. H. Dixneuf, A. J. Carty and N. J. Taylor, *Inorg. Chem.*, 1978, **17**, 2568.
- W. B. Person, K. G. Brown, D. Steele and D. Peters, *J. Phys. Chem.*, 1981, **85**, 1998.
- T. J. Collins, W. R. Roper and K. G. Town, *J. Organomet. Chem.*, 1976, **121**, C4.
- D. Touchard, J.-L. Fillaut, P. H. Dixneuf and L. Toupet, *J. Organomet. Chem.*, 1986, **317**, 291.
- D. H. Farrar and J. A. Luniss, *Acta Crystallogr., Sect. C*, 1985, **41**, 1444.
- L. J. Todd and J. R. Wilkinson, *J. Organomet. Chem.*, 1974, **77**, 1.

- 16 E. W. Abel, K. G. Orrell, H. Rahoo, V. Sik, M. A. Mazid and M. B. Hursthouse, *J. Organomet. Chem.*, 1992, **437**, 191.
- 17 N. E. Leadbeater, *Inorg. Chem.* in the press.
- 18 C. W. Bradford, W. van Bronswijk, R. J. H. Clark and R. S. Nyholm, *J. Chem. Soc. A*, 1970, 2889.
- 19 R. E. Benfield, B. F. G. Johnson, P. R. Raithby and G. M. Sheldrick, *Acta Crystallogr., Sect. B*, 1978, **34**, 666.
- 20 B. F. G. Johnson, J. Lewis and D. A. Pippard, *J. Chem. Soc., Dalton Trans.*, 1981, 407.
- 21 R. D. Adams and M. P. Pompeo, *Organometallics*, 1990, **9**, 1718.
- 22 P. A. Dawson, B. F. G. Johnson, J. Lewis, J. Puga, P. R. Raithby and M. J. Rosales, *J. Chem. Soc., Dalton Trans.*, 1982, 233.
- 23 M. R. Churchill and B. G. DeBoer, *Inorg. Chem.*, 1977, **16**, 868.
- 24 C. A. Tolman, *Chem. Rev.*, 1977, **77**, 313.
- 25 C. A. McAuliffe and W. Levenson, *Phosphine, Arsine and Stibine Complexes of the Transition Elements*, Elsevier, Amsterdam, 1979.
- 26 T. S. Cameron, P. A. Gardner and K. R. Grundy, *J. Organomet. Chem.*, 1981, **212**, C19.
- 27 D. H. Farrar, R. R. Gukathasan and K. Won, *J. Organomet. Chem.*, 1984, **275**, 263.
- 28 D. H. Farrar, R. R. Gukathasan and S. A. Morris, *Inorg. Chem.*, 1984, **23**, 3258.
- 29 H. Werner and K. Leonhard, *Angew. Chem., Int. Ed. Engl.*, 1979, **18**, 627.
- 30 P. V. Broadhurst, B. F. G. Johnson, J. Lewis and P. R. Raithby, *J. Am. Chem. Soc.*, 1981, **103**, 3198.
- 31 K. Kuchitsu and K. Oyanagi, *Faraday Discuss. Chem. Soc.*, 1977, 62; P. C. Cross and L. O. Brockway, *J. Chem. Phys.*, 1935, **3**, 821.
- 32 By reference to the Cambridge Crystallographic Database: F. A. Allen and O. Kennard, *Chem. Des. Autom. News*, 1993, **8**, 31.
- 33 B. F. G. Johnson and J. Lewis, *Inorg. Synth.*, 1976, **16**, 47.
- 34 A. C. T. North, D. C. Phillips and F. S. Mathews, *Acta Crystallogr., Sect. A*, 1968, **24**, 351.
- 35 G. M. Sheldrick, SHELXL 76, program for crystal structure determination, University of Cambridge, 1976.

Received 13th June 1997; Paper 7/04141A